

Electrochemical Impedance Spectroscopy of Li-Ion battery on-board the Electric Vehicles based on Fast nonparametric identification method

Original

Electrochemical Impedance Spectroscopy of Li-Ion battery on-board the Electric Vehicles based on Fast nonparametric identification method / Locorotondo, E; Pugi, L; Berzi, L; Pierini, M; Scavuzzo, S; Ferraris, A; Airale, A; Carello, M. - ELETTRONICO. - (2019). (19th IEEE International Conference on Environment and Electrical Engineering and 2019 IEEE Industrial and Commercial Power Systems Europe, IEEEIC/I and CPS Europe Genova 11-14 June 2019) [10.1109/IEEEIC.2019.8783625].

Availability:

This version is available at: 11583/2816964 since: 2020-04-28T16:22:35Z

Publisher:

IEEE

Published

DOI:10.1109/IEEEIC.2019.8783625

Terms of use:

This article is made available under terms and conditions as specified in the corresponding bibliographic description in the repository

Publisher copyright

IEEE postprint/Author's Accepted Manuscript

©2019 IEEE. Personal use of this material is permitted. Permission from IEEE must be obtained for all other uses, in any current or future media, including reprinting/republishing this material for advertising or promotional purposes, creating new collecting works, for resale or lists, or reuse of any copyrighted component of this work in other works.

(Article begins on next page)

Electrochemical Impedance Spectroscopy of Li-Ion battery on-board the Electric Vehicles based on Fast nonparametric identification method

E. Locorotondo*, L. Pugi, L. Berzi, M. Pierini

Department of Industrial Engineering
Università degli studi di Firenze,
Florence, Italy

*Corresponding author: edoardo.locorotondo@unifi.it

S. Scavuzzo, A. Ferraris, A.G. Airale, M. Carello
Department of Mechanical and Aerospace Engineering
Politecnico di Torino,
Turin, Italy

Abstract

Electrochemical Impedance Spectroscopy (EIS) is commonly used for the diagnosis of electrochemical energy accumulators, for example Li-Ion batteries in Electric and Hybrid Vehicles. Measuring the impedance in a wide frequency range, it is possible to investigate on the modifications of the internal electrochemical cell process, evaluating its current state of life. EIS test consists of the excitation of the battery, or cell, with a defined current signal, and then measuring the cell voltage, the frequency response of the system is computed. The classical EIS test, based on the excitation with a frequency controlled sine wave in input, requires expensive instruments and long time test procedures; therefore it has many problems on the integration on the embedded systems. In this paper, a pseudo random square signal, which shows a simply hardware implementation, is used as excitation signal input on the cell for the impedance evaluation. The effectiveness of the method has been validated based on simulation test, in order to obtain good results in terms of impedance estimation accuracy, minimizing time duration and energy consumption.

Keywords: *Li-Ion cell, EIS, Nonparametric identification, Periodic pseudo-random signals, Electric vehicles.*

I. INTRODUCTION

Monitoring and management of energy accumulators (rechargeable batteries) is one of the main themes of research and industrial development, mostly in the automotive field. Today, due to its power and energy density, high efficiency, long cycle life and low self-discharge, Li-Ion batteries have become considered as the most significant energy storage for Electric and Hybrid Vehicles (EV and HEV) applications. Nevertheless, Li-Ion batteries have a high cost and are more sensitive to working condition such as their usable capacity [1] and temperature [2], power demand and its lifetime due to aging [3]. Therefore, the continuous evaluation and prediction of battery performance and its service life (battery states) are significant requirements for consumers in automotive field. Monitoring battery status, the electronic control unit called Battery Management System (BMS) is usually employed in Li-Ion batteries, to perform reliable operations. Since batteries are complex electrochemical devices with a nonlinear behavior depending on various internal and external

For the University of Florence the project is a part of OBELICS project, which has received funding from the European Union's Horizon 2020 research and innovation programme under grant agreement No. 769506. For the Politecnico di Torino the project has been made thanks to the cooperation with Beond s.r.l.

conditions, and their monitoring is an important challenging task. In literature exist many mathematical methods for battery states evaluation [4].

The battery state is usually expressed as a vector which contains the following parameters:

- **State Of Charge (SOC):** is the percentage of residual capacity respect to battery nominal capacity.
- **State Of Health (SOH):** defines the battery performance degradation over time due unexpected events, always by considering variation in battery capacity or internal resistance.

Authors worked on online methods for battery SOC and SOH estimation, two examples are shown in [5] and in [6]. In particular, the dependence of battery impedance on the SOC and SOH has encouraged many researchers to investigate on this parameter. Due to complex electrochemical structure, battery impedance can take some different effects depending on its different dynamics, as visible in Nyquist plot in Fig.1. Analyzing in particular the shape of this curve, in the appropriate frequency range, SOC and SOH can be evaluated respectively in low frequency [7] and in high frequency [8]. Moreover, recent studies have shown that battery internal temperature can be directly measured based on impedance spectroscopy. Experimental test results prove that the zero-intercept Nyquist diagram frequency is exclusively related to the internal battery temperature [9]. This relationship does not depend on battery SOC and aging level, so impedance spectroscopy should be considered as a robust sensorless method for battery internal temperature measurement. Therefore, battery impedance provides useful information for current battery state.

Aim of this paper is the realization of an algorithm that evaluates the battery impedance in an appropriate frequency range. Main targets of the algorithm are the calculation of battery impedance in the shortest time with reduced computational costs and consumption, and therefore a possible implementation on board of the EV. A nonparametric identification method for battery electrochemical impedance spectroscopy has been realized, focusing in particular on broadband excitation signals, realized by periodic pseudo-random signals. The basis of battery impedance spectroscopy and the algorithm for battery impedance measurements have been developed, and, finally, the algorithm has been applied on the simulated data, where the results are compared with reference data.

II. ELECTROCHEMICAL IMPEDANCE SPECTROSCOPY

A. Theory

Electrochemical Impedance Spectroscopy (EIS) analyzes the chemical-physical property of electrochemical energy accumulator, in this work Li-Ion batteries. Measuring impedance in a wide frequency range, there is the possibility to analyze battery internal processes with different time constants [10]. It is important to clarify that these methods are mainly used to identify the model that describes the short-term behavior of the battery. Considering the battery as a Linear and Time-Varying (LTV) dynamic system, the general principle of impedance spectroscopy is to apply a sinusoidal signal in current i on the battery; measuring its voltage response v , battery impedance Z is computed by the equation:

$$Z = \frac{v(t)}{i(t)} = \frac{V \sin(\omega t + \varphi)}{I \sin(\omega t)} \quad (1)$$

Where: V and I are respectively the voltage and the current amplitude, ω is the angular frequency, φ is the phase shift. In the frequency domain, is possible to separate the impedance in a real part $Re(Z) = Re(Z(j\omega))$ and in a imaginary part $Im(Z) = Im(Z(j\omega))$ using the equation:

$$Z(j\omega) = Re(Z) + jIm(Z) = |Z| \cos(\varphi) + j |Z| \sin(\varphi) \quad (2)$$

Where: $\varphi = \varphi(j\omega)$, $j = \sqrt{-1}$. $Z = Z(j\omega)$ is the absolute value of the impedance, expressed by:

$$|Z| = |Z(j\omega)| = \sqrt{Re(Z)^2 + Im(Z)^2} \quad (3)$$

Real and Imaginary values of impedance should be displayed on Nyquist plot as shown in Fig.1; from it, mathematical battery model should be defined.

B. Battery modeling

Li-Ion cells show similar Nyquist plot as in Fig.1. Generally this plot can be divided in five sections, which describe particular internal processes at different time constants. There are many models to describe the behavior of a battery [4] but it is needed to use particular passive elements of an Equivalent Electrical Circuit (EEC) to simulate different five sections as shown in Fig.1 (above).

Starting from low frequency (right on Fig.1) and arriving to high frequency (left on Fig.1) it is possible to note:

- Warburg Impedance (W): considers the diffusion of Li-Ion in the porous active material of the electrodes: it can be simulated using a Warburg passive element w [8].
- Second RC group (R_2, CPE_2): R_2 is the resistance in the charge transfer occurring at the electrode surface; CPE_2 is the double layer capacity. The double layer is a region featuring a significant electric field between the electrode and the electrolyte acting like a capacitor [8]. This parameter is represented by a Constant Phase Element (CPE), a non-ideal capacity represented by an irrational transfer function, see [11] for further details.
- First RC group (R_1, CPE_1): considers the Solid Electrolyte Interphase (SEI) impedance film, which is created during cycling on the anode surface [8].
- Ohmic Resistance (R_{ohm}): its value is the sum of the resistance of current collectors, electrodes, electrolyte and separators [8]. An approximate value is the intersection between impedance curve and real axis.
- Inductance (L): at highest frequency, it shows the inductive behavior due to the metal elements of the cell and cables.

In the case of cell EIS, it is needed to simulate the same Nyquist plot using not simple capacity, but the Constant Phase Elements (CPEs). Indeed the impedance curve is not represented by a series of circle arcs, which should describe an ideal ohmic-capacitive behavior, but it is really represented by a series of ellipse arcs. More details about CPE and Warburg elements are shown in [8] and in [11].

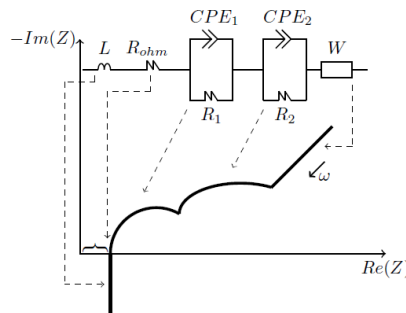


Fig. 1. Reference spectrum of Li-Ion cell in a wide frequency range and battery EIS modeling.

III. NONPARAMETRIC IDENTIFICATION METHOD

A. Assumption of LTI system

Since this paper mainly concerns EIS estimation algorithms and their implementation in embedded systems, only discrete-time models are discussed in this paper, where $n \in \mathbb{Z}$ is the time integer index. Considering the time interval $[0, N]$, cell system is supposed as a LTI system. If these assumptions are validated, the system can be characterized by frequency response, in the case of cell system by impedance response Z , using the Discrete Fourier Transform (DFT):

$$Z(k) = \sum_{n=0}^N z[n]e^{-j2\pi kn} \quad (4)$$

defined for the impedance signal z (impulse response) with a limited $N+1$ number of samples; $k \in [-1/2, 1/2]$ is the normalized frequency. If the system is BIBO-stable, i.e. $\sum_{n=0}^{N-1} |z[n]| < \infty$ the input i is a stationary process signal, the steady output response v is a stationary process signal with the input-output relationship:

$$\Phi_{vi}(k) = Z(k)\Phi_i(k) \quad (5)$$

where: $\Phi_i(k)$ is the Power Spectral Density (PSD) of input signal and $\Phi_{vi}(k)$ is the cross-PSD between input-output signals [12]. In (5), impedance transfer function should be estimated by the two PSD estimates.

B. Nonparametric identification algorithm and metrics for its validation

The general principle of this method is to excited the cell, considered as unknown LTI BIBO-stable system, with an appropriate current signal i , charactized as a stationary process. It is classified as an active Spectroscopy method [4], because it requires an appropriate circuit for active input signal generation. The idea of the algorithm is shown in Fig. 2. Measuring the cell output voltage v' , it is important to consider an additive measurement noise m . Finally the output of cell system is described as:

$$v'[n] = \sum_{p=-\infty}^{+\infty} (z[p]i[n-p]) + m[n] \quad (6)$$

In this paper, additive measurement noise is defined as a white Gaussian noise, which generates normally distributed random numbers with zero mean and an appropriate standard deviation (std) at each step time n . Infact, white noise contains a flat PSD in a wide frequency range. This is useful for the evaluation of the robustness of the impedance estimation method, because all frequencies are excited with the same noise power. Considering that the noise signals are uncorrelated with measurement signals, CPSD between two signals is equivalent to zero. Due to this last assumptions:

$$\Phi_{v'i} = \Phi_{vi} \quad (7)$$

Therefore, using Eq.(5), impedance should be estimated by the equations:

$$\hat{Z}(k) = \frac{\Phi_{v'i}(k)}{\Phi_i(k)} \quad (8)$$

$$\hat{\Phi}_m = \Phi_{v'} - \Phi_i \quad (9)$$

Eq (9) proves that impedance spectrum and output noise PSD can be estimated using only current and voltage cell measurement. In this case, authors consider only the additive noise in output measurement because input signal is realized using a known signal; moreover if an additive noise in

input measurement is considered, for impedance calculation need to know the noise value. CPSD and PSD can be easily calculated using periodograms PSD estimators. Welch estimator is a good choice for this work. The metric for frequency response estimation for a LTI system is the evaluation of the spectral coherence [12] between input i and output v' and it is defined as:

$$\gamma_{v'i}^2(k) = \frac{|\Phi_{v'i}(k)|^2}{\Phi_i(k)\Phi_{v'}(k)} \quad (10)$$

From the inequality $|\Phi_{v'i}(k)|^2 < \Phi_i(k)\Phi_{v'}(k)$ [13], it follows that the spectral coherence is bounded by 0 and 1. This statistical value evaluates the linear property of the system: so, if input i and output v' are linearly related, the coherence $\gamma_{v'i}^2 = 1$, and if i and v' are completely unrelated (linearly) $\gamma_{v'i}^2 = 0$. Moreover if the coherence function is greater than zero but less than one, i and v' may be in part linearly related, but in addition real system may contains other inputs, otherwise measurements acquired may be noisy. Indeed, from (9) and (10), noise output PSD depends on output PSD and coherence result:

$$\hat{\Phi}_m(k) = (1 - \gamma_{v'i}^2(k))\Phi_{v'}(k) \quad (11)$$

Finally, it has been shown in [14] that variance of the gain $|\hat{Z}|$ and phase $\hat{\phi}$ impedance are directly related to spectral coherence by the equation:

$$\text{Var}(\hat{\phi}(k)) = \text{Var}(\ln(|\hat{Z}(k)|)) = \frac{1}{2L_w} \left(\frac{1}{\gamma_{v'i}^2(k)} - 1 \right) \quad (12)$$

Using Welch PSD estimator, measurement signals are splitted in L_w segments (window) of length N_w ; then are calculated the Fast Fourier Transform (FFT) of L_w segments. Finally the FFT mean values are computed. By Eq (12) it is proven that an higher spectral coherence consists of a lower estimation error. Moreover, an higher value of windows L_w consists on lower estimation error, but an higher calculation time.

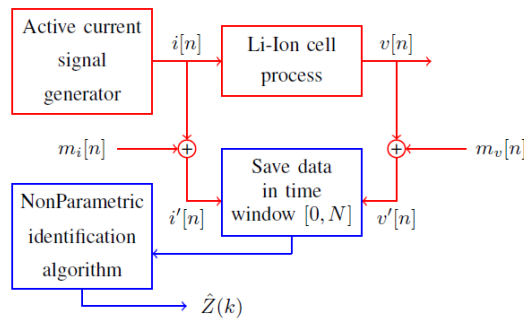


Fig. 2. Active Impedance spectroscopy method: red acquired measurement and blue computed data-set.

C. Excitation signal classes

Broadband excitation signals [14]-[15] are usually used as input in the active Impedance spectroscopy in Fig.2, in order to obtain the maximum informations about the system behavior in the excited frequency band. There are, three different classes of signal used in frequency response estimation of a LTI system [15]:

- **Random signals:** white noise.
- **Transient signals:** pulse, burst sine, burst random.

- **Periodic signals:** Periodic Multisine, Pseudo-Random.

The white noise presents a flat PSD over all frequencies; however its signal generation requires a complex hardware realization. Moreover it suffers of leakage problem [15]-[16], so a probability of a highly reduced Signal to Noise Ratio (SNR) at some randomly located frequencies. Pulse signals are used for fast system identification and they shows a simply hardware implementation. However they present an high crest-factor, inducing to high energy consumption during impedance estimation. Periodic signals are more used in fast system identification. In particular, multisine signals offers various advantages in the detection of nonlinear distortion. Then it becomes a good instrument if we want to study separatly linear and nonlinear behavior of the system, as shown in [16]. Instead, periodic pseudo-random signals are optimum for perfect linear and slightly nonlinear system identification. The main target of the realized algorithm for the fast and accurate impedance spectroscopy evaluation is to excite the cell affecting SOC as little as possible (less energy consumption). Therefore to maintain the conditions under which the cell can be approximated by the LTI system. Finally it is important to realize an excited broadband signal which presents a simple hardware implementation. The periodic pseudo-random signal satisfy these requirements, and in the next section it is introduced in details.

D. Pseudo Random Binary Square (PRBS)

PRBS signal is one of the more popular input signal used in nonparametric identification. It is a discrete-time periodic pseudo-random signal that switches between two logic levels: therefore it is a square wave signal. One of the biggest advantages of this signal is the simply hardware implementation: PRBS can be generated using only a certain number of shift registers, block system is shown in Fig.3. The generation of the current PRBS signal requires to select the two amplitude levels and the period of the signal, which is equivalent with $M = 2^{n_r} - 1$, where n_r is the number of shift registers. Furthermore, the clock period T_c is required, i.e. the minimum number of sampling intervals which allows the PRBS sequence to switch. The discrete-state variables $x_k[n]$ are binary values (0 or 1). At each clock instant time nT_c , the k_b -th state is transferred to $(k_b + 1)$ -th state:

$$x_{k_b+1}[n] = x_{k_b}[n], \quad k_b = 1, \dots, n_r - 1 \quad (13)$$

$$i[n] = x_{n_r}[n] \quad (14)$$

The new value of the state $x_k[n+1]$ is obtained in feedback, see Fig.3, using the modulo-2 addition ($\text{rem}(\cdot, 2)$), considering the gain factors $g_k \in \{0,1\}$, for $k = 1, \dots, n_r$:

$$x_k[n+1] = \text{rem}\left(\sum_{k=1}^{n_r} g_k x_k[n], 2\right) \quad (15)$$

The interesting property of PRBS signal [12] is the following:

$$R_i(\tau) = \frac{1}{M} \sum_{n=1}^M i[n]i[n+\tau] = \begin{cases} A^2 & k = 0, \pm M, \pm 2M \dots \\ -\frac{A^2}{M} & \text{else} \end{cases} \quad (16)$$

It's noticeable that if the period of the PRBS M is bigger, the function is more near that white noise auto-covariance. R_i is not exactly the auto-covariance function of PRBS signal, because its mean value is not exactly zero. Nevertheless, in frequency domain, considering M value bigger, so increasing the number of the shift registers n_r , PSD of PRBS signal is similar to white noise PSD, as shown in Fig.4.

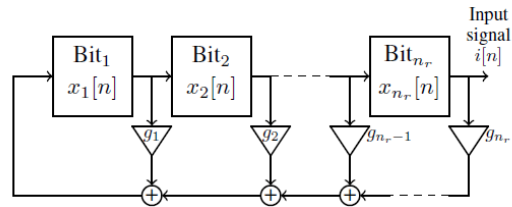


Fig. 3. PRBS signal generator's circuit.

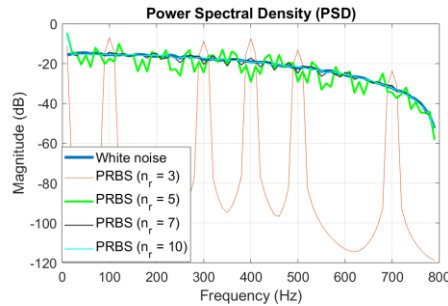


Fig. 4. PSD function of PRBS signal using different number of shift registers, simulated in Matlab/Simulink.

IV. RESULTS

Cell EIS estimation's effectiveness using nonparametric identification method, based on PRBS current signal excitation, is evaluated during many simulation test on EEC model in Fig.1 (above).

A. *Experimental setup*

The evaluation of cell model parameters are performed on a specific LiFePO₄ cell from A123, the ANR26650M1-B (2.5 Ah of capacity and 3.3 V of nominal voltage). Cell model parameters (Fig.1) are estimated fitting the EIS data measurement, in the frequency range (10-100 Hz), and are shown in Table I. In this work, the CPEs have been replaced by pure capacities (C_1, C_2), obtaining an excellent fit with the experimental EIS data. Finally, the Equivalent Electrical Circuit (EEC) model is implemented in Matlab/Simulink Software. The electronic load MM540 by Material Mates Instruments has been used to spectroscopy test. The instrument has a dedicated frequency response analyzer that produces the excitation signals. The instrument is connected to a personal computer (PC) through USB protocol. The PC drives the instrument by means of a dedicated software and simultaneously collects the measurements and calculates the EIS (Fig.5).

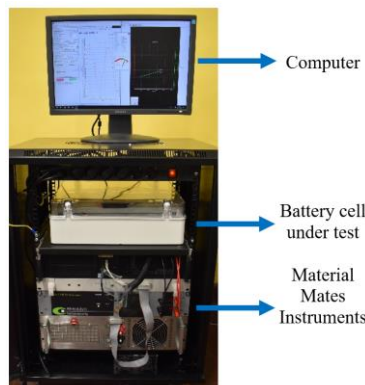


Fig. 5. Laboratory EIS test setup.

TABLE I
EEC CELL MODEL PARAMETERS AT SOC 70%

Parameter	Value	Description
L	6 [mH]	Inductance
R_{ohm}	37 [mΩ]	Ohmic Resistance
R_1	0.8 [mΩ]	SEI Resistance
C_1	6 [F]	SEI Capacity
R_2	0.5 [mΩ]	Charge Transfer Resistance
C_2	55 [F]	Double Layer Capacity

B. Test Data

The implementation in Matlab/Simulink of EEC model simulates the behavior of LiFePO4 cell receiving current signal in input. As mentioned before, estimating its frequency response, model must be considered as LTI system during the whole measurement time. Therefore, using appropriate duration time and PRBS amplitude level, SOC variation must be very little, especially in the extreme parts of the SOC window. In this work, initial cell SOC is 70% and the duration time is chosen in order to discharge cell on 2%. The PRBS discharge current signal is generated with peak level of 0.3C, 0.5C, 1C, 2C-rate, the number of shift registers is $n_r = 10$, the clock frequency is $f_c = 800$ Hz. A current offset of 0.2 A is added to the signal to keep the cell always in phase discharging during test measurement, avoiding the hysteresis non-linearity effect between charging/discharging phase [17]. Current and cell voltage are acquired at sampling frequency $f_s = 8000$ Hz and cell impedance is estimated in the frequency range of (10-100 Hz), with a frequency resolution $f_r = 2$ Hz. Consequently, using Welch periodogram estimator, measurement signals are splitted up into a certain number of L_w disjoint (no overlap) segments of $N_w = f_s / f_r = 1600$ samples, which are the FFT points to use in PSD estimate. It's noticeable that the PRBS signal presents an almost flat PSD spectrum over the frequency band f_c . However, as shown in Fig.6, PRBS signal induces a significant decrease in the upper frequency band. Therefore, in order to maintain the spectrum coherence near to 1, more restricted frequency range (10-100 Hz lower frequency) is used in this paper.

C. Evaluation of Nonparametric Identification method

The impedance estimation performance using the nonparametric identification method is evaluated. The robustness of the algorithm is evaluated adding a voltage measurement noise as shown in Fig.2. The noise is defined as a white Gaussian noise, with zero mean and standard deviation $\sigma_v = 5$ mV. To study the influence of the voltage noise measurement on algorithm, 100 simulation test are performed for each PRBS peak level. The metric for the evaluation of the gain and phase impedance estimation's effectiveness used in this work is the Root Mean Square Error's Percentage (%), defined by the equation:

$$RMSEP = \sqrt{\frac{1}{N_{tot}} \sum_{k_f=f_{min}}^{f_{max}} \left(\frac{\hat{Z}(k_f) - Z(k_f)}{Z(k_f)} \right)^2} \times 100 \quad (17)$$

This statistical value is calculated during each single test simulation using the N_{tot} sample impedance data estimated: $Z(k_f)$ and $\hat{Z}(k_f)$ are respectively the reference and estimated impedance at frequency k_f , where $k_f \in [f_{min}, f_{max}]$ Hz, with frequency resolution f_r . Moments of RMSEP (mean and std) are computed for each PRBS peak level and results are shown in Table II. It's noticeable that the gain impedance estimation differs at least one order of magnitude respect to phase impedance estimation. Moreover the time duration for measurement data acquisition used by the algorithm is computed in order to maintain a discharged SOC about 2%, ensuring the LTI system's assumption and low energy consumption. Finally, for lower current peaks, the increase of the time duration is required, for an accurate impedance estimation. Nevertheless, the impedance estimate is more accurate using higher current peaks. Indeed, the excitation signal with higher amplitude induces an higher Signal to Noise Ratio (SNR) in output. In Fig. 8 it is shown that the nonparametric identification method reaches more accurate impedance estimation when the SNR is higher. Further considerations should be made for frequency resolution f_r : at the same time duration, better frequency resolution induces to a reduction of number of disjoint segments L_w . Therefore a reduction of windows consists on an higher RMSEP, as shown in Fig.8.

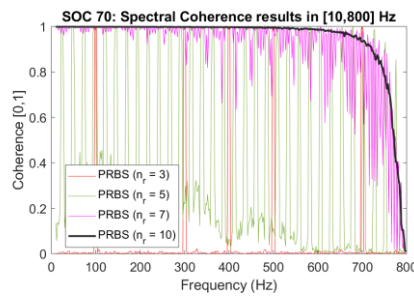


Fig. 6. Coherence results using different number of shift registers, resolution 2 Hz, and additive voltage white noise with zero mean and $\sigma_v = 5$ mV.

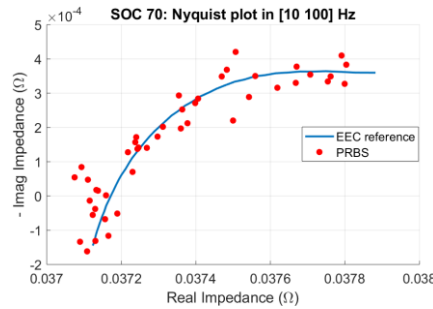


Fig.7. EIS result using PRBS current signal with peak level 1C, resolution 2 Hz, additive voltage white noise with zero mean and $\sigma_v = 5$ mV.

TABLE II
ALGORITHM PERFORMANCE FOR EIS ESTIMATION, CONSIDERING ADDITIVE WHITE NOISE VOLTAGE WITH ZERO MEAN AND σ

PRBS peak	Test time (s)	Discharged SOC (%)	Gain RMSEP $ \hat{z} $		Phase RMSEP $\hat{\phi}$	
			Mean (%)	Std (%)	Mean (%)	Std (%)
0.3 C	350	2.01	0.37	0.05	3.60	1.54
0.5 C	240	2.04	0.23	0.03	2.38	1.06
1 C	125	2.03	0.14	0.02	1.31	0.63
2 C	65	2.04	0.10	0.01	0.94	0.46

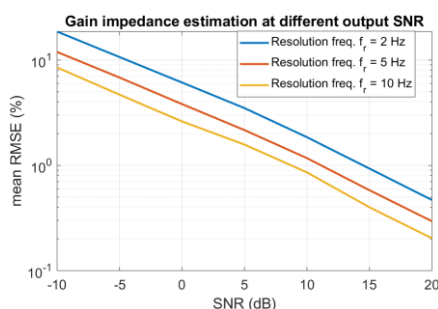


Fig.8. Gain impedance RMSE at different output SNR and different resolution's frequency.

V. CONCLUSIONS

This paper has shown a nonparametric identification method to identify the cell impedance spectroscopy, focusing on the broadband signals, in particular on the periodic pseudo-random types. Firstly, algorithm has been theoretically introduced, considering the assumption of the LTI property the cell system. Simulation results indicate that the performance of impedance estimation in a defined frequency band has shown good results in terms of accuracy, time duration and energy consumption. In particular the algorithm reaches better results when the output SNR is higher. Based on these results, possible future developments should be the implementation of this algorithm on board the Electric Vehicle for Li-Ion battery monitoring.

REFERENCES

- [1] D. Cittanti, A. Ferraris, A. Airale, S. Fiorot, S. Scavuzzo, and M. Carello, "Modeling Li-ion batteries for automotive application: A trade-off between accuracy and complexity," International Conference of Electrical and Electronic Technologies for Automotive, Torino 15-16 June 2017, pp.8,2017,ISBN:978-88-87237-26-9,DOI: 10.23919/EETA.2017.7993213.
- [2] De Vita A., Maheshwari A., Destro M., Santarelli M., Carello M., "Transient thermal analysis of a lithium-ion battery pack comparing different cooling solutions for automotive applications", Applied Energy, Vol.206,pp.12,2017,ISSN:0306-2619, DOI:10.1016/j.apenergy.2017.08.184.
- [3] S. Scavuzzo, R. Guerrieri, A. Ferraris, A. Giancarlo Airale and M. Carello, "Alternative Efficiency Test Protocol for Lithium-Ion Battery," IEEE International Conference on Environment and

Electrical Engineering and IEEE Industrial and Commercial Power Systems Europe, IEEEIC/ and CPS Europe 2018, Palermo 12-15 June 2018, ISBN: 978-153865185-8, DOI: 10.1109/IEEEIC.2018.8493664.

- [4] W. Waag, C. Fleischer, and D. U. Sauer, "Critical review of the methods for monitoring of lithium-ion batteries in electric and hybrid vehicles." *Journal of Power Sources* 258 (2014): 321-339.
- [5] E. Locorotondo, L. Pugi, L. Berzi, M. Pierini and G. Lutzemberger, "Online Identification of Thevenin Equivalent Circuit Model Parameters and Estimation State of Charge of Lithium-Ion Batteries," 2018 IEEE International Conference on Environment and Electrical Engineering and 2018 IEEE Industrial and Commercial Power Systems Europe (IEEEIC / I&CPS Europe), Palermo, 2018, pp. 1-6.
- [6] E. Locorotondo, L. Pugi, L. Berzi, M. Pierini and A. Pretto, "Online State of Health Estimation of Lithium-Ion Batteries Based on Improved Ampere-Count Method," 2018 IEEE International Conference on Environment and Electrical Engineering and 2018 IEEE Industrial and Commercial Power Systems Europe (IEEEIC / I&CPS Europe), Palermo, 2018, pp. 1-6.
- [7] J. Gomez, R. Nelson, E. Kalu, M. Weatherspoon, and J. P. Zheng, "Equivalent circuit model parameters of a high-power Li-ion battery: Thermal and state of charge effects" *Journal of Power Sources*, 196(10), 4826-4831, 2011.
- [8] Y. Olofsson, J. Groot, T. Katrašnik, e G. Tavcar, "Impedance spectroscopy characterisation of automotive NMC/graphite Li-ion cells aged with realistic PHEV load profile", in *Electric Vehicle Conference (IEVC)*, 2014 IEEE International, pp. 1–6, 2014.
- [9] L.H.J. Rajimakers, D.L. Danilov, J.P.M. van Lammeren, M.J.G. Lammers, P.H.L. Notten, "Sensorless battery temperature measurements based on electrochemical impedance spectroscopy," *Journal of Power Sources*, vol. 247, pp. 539-544, 2014.
- [10] D. Andre, Meiler, K. Steiner, C. Wimmer, T. Soczka-Guth, and D. U. Sauer, "Characterization of high-power lithium-ion batteries by electrochemical impedance spectroscopy. I. Experimental investigation" *Journal of Power Sources*, 196(12), 5334-5341, 2011.
- [11] F. Berthier, J.P Diard, R. Michel, "Distinguishability of equivalent circuits containing CPEs: Part I. Theoretical part." *Journal of Electroanalytical Chemistry*, 510(1-2), 1-11, 2001.
- [12] L. Ljung, "System Identification - Theory for the User", Prentice Hall, 1999.
- [13] J. Silva and N. Maia, "Modal Analysis and Testing", Applied Science, Vol. 363, 1999.
- [14] R. Al Nazer, V. Cattin, P. Granjon, M. Montaru and M. Ranieri, "Broadband Identification of Battery Electrical Impedance for HEVs," in *IEEE Transactions on Vehicular Technology*, vol. 62, no. 7, pp. 2896-2905, Sept. 2013.
- [15] D.J. Ewins "Modal testing: theor, practice and application, 2nd edition", ResearchStudies Press Ltd, 2009.
- [16] R. Relan, Y. Firouz, J. Timmermans and J. Schoukens, "Data-Driven Nonlinear Identification of Li-Ion Battery Based on a Frequency Domain Nonparametric Analysis," in *IEEE Transactions on Control Systems Technology*, vol. 25, no. 5, pp. 1825-1832, Sept. 2017.
- [17] T. Huria, G. Ludovici, G. Lutzemberger, "State of charge estimation of high power lithium iron phosphate cells", *Journal of Power Sources*, Volume 249, Pages 92-102, 1 March 2014.